

Micro-arcsec imaging from the ground with intensity interferometers

Aviv Ofir^{a,1}, and Erez N. Ribak^b

^aAstronomy Dept, Tel Aviv University, Tel Aviv 69978 Israel;

^bPhysics Dept., Technion, Haifa 32000, Israel

ABSTRACT

Stellar amplitude interferometry is limited by the need to have optical distances known to a fraction of the wavelength. We suggest reviving intensity interferometry, which requires far less accurate hardware (~1cm mechanical precision) at the cost of more limited sensitivity. We present an algorithm that uses the very high redundancy of a uniform linear array to increase the sensitivity of the instrument by more than a hundredfold. An array of a hundred ~100m diameter elements can achieve a limiting magnitude of $m_b=14.4$. Off-line processing of the data will enable such a ground-based facility to transform a two-dimensional field of point-like sources to a three-dimensional distribution of micro-arcsec resolved systems, each imaged in several optical bands. Each system will also have its high resolution residual timing, high quality (inside each band) spectra and light curve, emergent flux, effective temperature, polarization effects and perhaps some thermodynamic properties, all directly measured in a single observation run of such a dedicated facility. Coronagraphy, selectively suppressing large scale structures of the sources, can also be achieved by specific aperture shapes. We conclude that after three decades of abandonment optical intensity interferometry deserves another review, also as a ground-based alternative to the science goals of space interferometers.

Keywords: instrumentation: interferometers - instrumentation: high angular resolution - techniques: interferometric

1. INTRODUCTION

Amplitude (or Michelson) interferometry is today's mainstream technique for high angular resolution astronomy. Amplitude interferometers add the complex amplitude of the electromagnetic waves from two or more separate locations to produce a high-resolution brightness distribution, or image, of the source. Intensity interferometry, on the other hand, "interferes" the intensities of the electromagnetic wave via the correlation of the electrical currents generated by the detectors of the already-detected intensities. The main advantage of intensity interferometry is its mechanical robustness: the required opto-mechanical accuracy depends on the electrical bandwidth of the detectors and not on the wavelength of the light, and thus the mechanical precision required is relaxed by many orders of magnitude. This low path-length sensitivity also means that the existence of an atmosphere does not influence the performance of the instrument. The main disadvantages of intensity interferometry, which led to its demise, are its very low intrinsic sensitivity and the fact that the classical, two-detector intensity interferometer can not reconstruct the phase of the complex degree of coherence, and thus cannot be used to produce true images¹.

Development of the two-detector stellar intensity interferometer started in radio astronomy², but was expanded to the optical regime^{3,4} to culminate in the measurement of the angular diameter of 32 stars, during the operation of the Narrabri Stellar Intensity Interferometer (NSII) from 1965 to 1972. The low sensitivity prohibited observing stars fainter than $m_b=2.5$ though NSII used a pair of 30m² reflectors¹. In fields other than astronomy intensity interferometry has been applied to nuclear physics (usually called "HBT effect")⁵, ultra short laser pulses⁶, characterization of the synchrotron radiation⁷, hard disks head-disk spacing measurement⁸, and measurement of electron temperature fluctuations in fusion plasmas⁹. It even seems that Fluorescence Correlation Spectroscopy (FCS), a technique regularly used in biology and chemistry, is actually intensity interferometry in disguise, and this similarity is especially striking when comparing works on FCS¹⁰ and triple correlation^{11,12}. The considerations in this paper apply not just in astronomy but wherever intensity interferometry is used.

Gamo¹³ first proposed and Sato *et al*¹⁴ proved experimentally that the three-detector intensity interferometer, which correlates the intensities from three separate detectors, can reconstruct the phase of the complex degree of coherence. Later, more algorithms to reconstruct the missing phase of the complex degree of coherence from amplitude-only

¹ Address for correspondence: avivofir@wise.tau.ac.il

measurements were proposed, by using second-, third-, and fourth order intensity correlations¹⁵, triple correlations and bispectra^{11,12,16}, fractional triple correlation¹⁷, and even by using just the usual second-order correlations and the Cauchy–Riemann equations¹⁸.

Fontana¹⁹ generalized intensity interferometry to N detectors correlating all N currents to form a single output. We adopt Fontana’s notations: the multiple correlation function $F^{(N)}(\tau_1, \tau_2, \dots, \tau_N) = \int_{-\infty}^{\infty} \langle I_1(t - \tau_1) \dots I_N(t - \tau_N) \rangle dt$ and its excess above the zero-coherence term $\int_{-\infty}^{\infty} \langle I_1(t - \tau_1) \rangle \dots \langle I_N(t - \tau_N) \rangle dt$ which will be designated $\Delta F^{(N)}$. As Fontana, we notate the first order correlation function as $g_j(\tau)$, where τ_i are the electrical delays added to each beam. We note that Fontana correlated *all* currents to form a *single* output, so Fig. 1 in ref. 19 is somewhat misleading.

2. REDUNDANCY TO INCREASE SNR

Firstly we describe the proposed instrument: we define reflectors as the surfaces of light collection and detectors as the series of the light-detecting instruments observing a *single* source. Mounted on each reflector there may be several detectors, each observing a different source where all the j detectors onboard each of the N reflectors point at the same source. In contrast with Fontana’s N -detector intensity interferometer we record all signals directly after the amplifiers, and perform all correlations off-line, by software (Fig. 1). This setup will make it easier for us to use each signal many times, and to perform all other algorithms on the data at any later time.

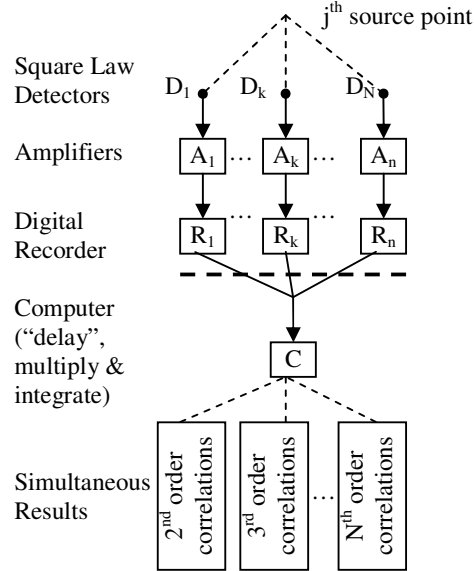


Fig. 1: In our intensity interferometer the correlations are performed off-line, by software.

We will now show that for a linear array of many detectors with a uniform spacing d there is much more redundancy than one might naively think, and that this high redundancy can be used to effectively increase the overall signal to noise ratio (SNR). In general, one can compute not just the second order intensity correlation between detectors a and b , $F^{(2)}(\tau_a, \tau_b)$, but also the m^{th} order correlation, $F^{(m)}(\{m\})$, of any m -sized subgroup of detectors $\{m\}$. The signal from each higher order of multi correlation $F^{(m)}(\{m\})$ will grow smaller with m . Still, the very high redundancy of $F^{(m)}(\{m\})$ will sometimes more than compensate for this. There are two types of redundancy: translational symmetry and high order expressions:

- (1) From translational symmetry, one can see that any pair (a, b) of detectors with a baseline of $|a-b|d$ is identical to any other pair of the same separation, and there are $N-|a-b|$ such pairs. Unlike amplitude interferometry, they can be added directly, since all phase information is already lost after detection.
- (2) In the case of fields that obey Gaussian statistics, like stellar light, all high moments of the multi-correlation function (3rd and higher) can be expressed as a function of the first- and second- order correlations. This means that:
 - a. The analytical expression for the correlation of m detectors – a, b and $(m-2)$ other detectors – is the m^{th} -order ($m>2$) correlation $F^{(2)}(\tau_a, \tau_b, \dots, \tau_m)$, and it can be expressed as a function of low order correlations that will also include the specific expression $F^{(2)}(\tau_a, \tau_b)$.
 - b. Reversing this relation, from each new subgroup one can construct a new expression of $F^{(2)}(\tau_a, \tau_b)$ by using the new $F^{(2)}(\tau_a, \tau_b, \dots, \tau_m)$.
 - c. Since there are $G = \binom{N-2}{m-2}$ subgroups of N with m members of which two are exactly a and b , there are also G different expressions for $F^{(2)}(\tau_a, \tau_b)$ in all subgroups of m members of N detectors.
 - d. Since the number of subgroups of m elements of N peaks at $m=N/2$ while the signal from every higher order correlation is increasingly smaller, there is no gain in continuing beyond $m=N/2$.

Combining (1) and (2), the number of expressions of $F^{(2)}(\tau_a, \tau_b)$ possible with all $F^{(m)}(\{m\})$, or the redundancy of $F^{(2)}(\tau_a, \tau_b)$ in all subgroups of N is:

$$\sum_{m=2}^{\lfloor N/2 \rfloor} \binom{N-2}{m-2} (N-|a-b|) \quad (1)$$

Thus giving a very high incentive to increase the number of reflectors N . In a separate paper we gave the full mathematical treatment giving the instrument's total SNR as a function of all the relevant parameters²⁰. We also introduced in the same paper a "coronagraphic" effect of intensity interferometry which can be used to increase the dynamic range of the instrument even further, but this effect was not thoroughly explored and is not included in the results below. In essence, it appears that the N -detector intensity interferometer can operate in a regime where the SNR scales approximately *exponentially* with the product $NA\alpha n$, where A is the area of each reflector, α is the detector's quantum efficiency and n is the spectral photon flux density of the source. Specifically, if the optical bandwidth is narrow enough so that both α and n are constant for all relevant frequencies ν , the resultant SNR of any subgroup of m detectors is proportional to

$$SNR \propto (A\alpha n)^{m/2}. \quad (2)$$

3. SIMULATIONS AND PROJECTED CAPABILITIES

3.1. Results and Analysis

To compute real-world results we used the NSII performance figures¹: wavelength $\lambda = 438.4\text{nm}$, electrical bandwidth $b_e = 100\text{ MHz}$, quantum efficiency $\alpha = 0.2$, system efficiency $\mathcal{S} = 0.2$, and reflectors area $A = 30\text{ m}^2$, to achieve $SNR = 27$ for integration time $T_0 = 1\text{ hr}$ of a star of blue band magnitude $m_b = 0$ (i.e. a photon flux density of $n = 5 \cdot 10^5\text{ photons m}^{-2}\text{ sec}^{-1}\text{ Hz}^{-1}$). The fact that the technological parameters scaling laws are experimentally verified will also allow us to correctly allow for all technological improvements since 1972.

Since we know that the redundancy of $\{m\}$ in Eq. (2) is highly dependant on N , we investigated the effect of the quantities in question. Since the quantum efficiency α has a relatively narrow range to change, we continue and change $A \cdot n$ (namely the photon flux density at each detector). In some non-astronomical applications n is controllable, and increasing it will give similar results to increasing A , since what matters is the product $A\alpha n$. In astronomy n is

uncontrolled, and Eq. (2) means a strong incentive to choosing the wavelength in which n is maximal for each source. We will therefore use the number of reflectors N and the area of the single reflector A as the main variables in our analysis (see Section 4 for discussion on the case when apertures A can no longer be considered “small”).

In Fig. 2 we plotted the SNR of the correlation function for $1d$ separation of several offline, multi-detector, linear and uniform intensity interferometers, each with a different (but uniform) reflector area A , as a function of the number of reflectors in the array N . The individual reflectors’ area starts at 30m^2 (as in NSII) and double the effective linear size (quadruple A) at each new plot up to an area of 7680m^2 , or a single reflector diameter of $\sim 100\text{m}$ (similar to current Extremely Large Telescope concepts, but our reflectors are crude light buckets and not telescopes). A clear change in behavior is evident on the 7680m^2 plot around $N \approx 10-20$, and a similar, more subtle, change can be seen on the 1920m^2 plot (near $N \approx 50-60$). These plots *do not* illustrate technological dependence, being taken to be the same as those of NSII.

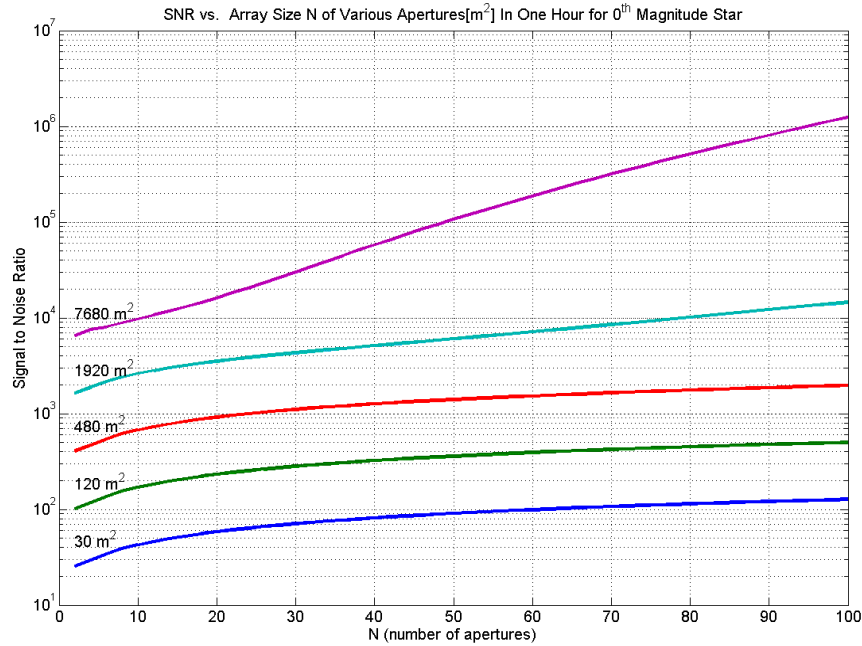


Fig. 2. The SNR of different arrays, all using NSII technology, each with a different aperture as indicated, vs. N for a separation $|a_1 - a_2| = 1$ in one hour for a star of 0 magnitude. Apertures range from 30m^2 (as in NSII) to 7680m^2 . A clear change in behavior is seen on the 7680m^2 plot, and a similar, more subtle, change can be seen on the 1920m^2 plot (around $N=54$).

The leftmost point ($N = 2$) on the 30m^2 (bottom) plot is the known NSII performance quoted at the end of §3.1. The uniform (on log scale) spacing between all the left-most points of each plots (all $N=2$) demonstrates the known linear scaling law of the two-detector intensity interferometer with respect to reflectors’ area¹.

The entire 30m^2 plot illustrates the 4.91 fold improvement (over the 2-element instrument) of the SNR of when we simulated a 100-element intensity interferometer, each of them identical to the ones used by NSII. This curve is entirely the result of the translational redundancy symmetries of different pairs - there are no observable differences if one ignores all higher order contributions.

Let us now explain the shape of the upper plots of Fig. 2: The overall behavior of all the plots with respect to N is tapering down with increasing N – the translational symmetry behavior. Apart from this behavior, the change in behavior of the 7680m^2 plot implies that a new element becomes important around $N \approx 10 - 20$. Since we already know that the 30m^2 plot is entirely the product of the usual second order correlations (no contribution from high orders) we shall call that change in behavior a transition from “two-correlation regime” to “multi-correlation regime”. We will now find the condition in which the contribution of all pairs is equal to that of all next-level correlations, i.e., all triplets. In §2.1 we

showed that the redundancy of all subgroups of size m is $\binom{N-2}{m-2} \binom{N-|a_1-a_2|}{m-2}$ while signal from each of these subgroups is proportional to $(A\alpha n)^m$, giving a total signal from all subgroups of certain size m :

$$\binom{N-2}{m-2} \binom{N-|a_1-a_2|}{m-2} (A\alpha n)^m \quad (3)$$

Comparing this expression for $m=2$ (pairs) and $m=3$ (triplets) will give us an N - A relation determining when one should see the contribution from all triplets equal to that from the pairs. For the separation of $|a_1 - a_2| = 1$ depicted in Fig. 2, we get $(N-2)A\alpha n = 1$ which means that an array with reflector size $A=7680\text{m}^2$ and a 0 magnitude star will be dominated by triplets when $N = 15.02$, or alternatively, that an array of 15 detectors will be triplets-dominated for reflector sizes of 7692m^2 and up. This procedure can be applied to also check when the quadruples start to contribute even more than the triplets, which happens at $N = 29$, and quintuplets will contribute more than the quadruplets at $N = 43$, sextuplets will dominate at $N = 57$, septuplets at $N = 71$, octuplets at $N = 85$ and finally nonuplets at $N = 99$. The end result is such a long exponential rise because it is actually the stacking of all the above contributions. Similarly, a transition to triplets domination, although not as pronounced, can be observed also for the $A = 1920\text{m}^2$ around $N = 54$. Now we can explain why no such transition has been observed at the lower area plots, like the 30m^2 plot, as the transition point for triplets domination for it is at $N = 3335$, and for the 480m^2 plot the transition point is at $N = 210$.

This behavior is almost completely technology-independent, but the absolute values are very much effected by technology: an estimate for the technological improvements since 1972 give, with the scaling laws given in ref. 1, a 40 fold improvement by conservatively changing b_ν to 1GHz, α to 0.8, Σ to 0.8, and still only one optical channel, $p=1$. We choose not to pursue the technological options further here, but we note that a measure to the conservatism in our estimate is the 1969 paper by Twiss arguing that technology alone could increase the SNR for the two-detector intensity interferometer by a factor of 80²¹.

Dimmer sources affect the result in a way similar to smaller reflectors since SNR of any subgroup is proportional to $(A\alpha n)^m$. Following Hanbury Brown and Twiss, we define the limiting magnitude of the instrument as the magnitude where we only get SNR of 3 after one hour of integration, then the limiting magnitude of the 7680m^2 , 100 element off-line intensity interferometer is slightly more than the 10th magnitude using the NSII technology, and about 14.4 magnitudes when the above mentioned conservative technological improvements are considered. At that point one will notice that: (i) Redundancy from translational symmetry do not depend on the source's strength, so this effect remains and contributes (see the behavior of the lower plots of Fig. 2). (ii) Redundancy from higher order correlations is highly dependant on the photon flux n , and its contribution is negligible for sources dimmer than magnitude 3 for the $\sim 100\text{m}$ diameter reflectors (using NSII technology). Virtually all the instrument's capabilities beyond this point are due to the shear area of the reflectors and the translational symmetry. (iii) In calculating the preceding figures we did not include the coronagraphic effect (see §4) as it depends also on the source's angular size and the reflector's shape, and can thus be chosen to have a modest impact.

4. CORONAGRAPHY WITH LARGE APERTURES

In what appears to be in some conflict with our computations here, the SNR cannot be indefinitely increased simply by increasing the reflector size A . Intensity interferometry is based upon the assumption that the source is a "point" source (i.e., smaller than the diffraction limit of a single reflector). By increasing the reflectors to very large diameters one realizes that some stars can no longer be considered as point sources. This effect was accounted for by Hanbury Brown and Twiss by introducing the partial coherence factor $\Delta(\nu)$ ⁴ which reduces the observed correlation for partially resolved sources, cancels the observed correlation altogether for completely resolves sources, and complicates the interpretation considerably as $\Delta(\nu)$ also depends on the size and shape of the source.

Yet, we foresee a way to utilize that effect to our advantage for searching and characterizing extremely high dynamic range objects, like binaries, multiples and even extra-solar planets: when one observes an extra-solar planetary system around sun-like stars one notices three length scales: the orbital distances of the planets, the size of the star and the sizes of planets. If we choose a reflector size between the size needed to resolve the star and the planets, we would find that $\Delta(\nu)$ has already significantly reduced the stellar signal, but it has yet to affect the planetary signals. By "using" the

partial coherence factor we can selectively attenuate the signal from all large scale structures of the source (which are almost always the brighter structures), and don't need dynamic range as wide as before, which means that our instrument is now also a coronagraph. This quality of the large-aperture intensity interferometers enables one to apply coronagraphy to stars other than the Sun, and to do it from the ground. We clarify that this effect will reduce the signal from object scales close to- and larger than- the diffraction limit of the single dish, and not from object scales close to the diffraction limit of the baseline.

For example, for a 7680m² square shaped reflector observing a star like the sun at a distance of 10pc, the partial coherence factor of 0.72 reduces the pair-wise correlation (stellar signal) by 28%. This modest attenuation can be enhanced by considering elongated or rectangular reflectors. It doesn't matter which side is longer as long as the round symmetry of the object is not broken. For the same reflector area, this setup will reduce the pair-correlation stellar signal by a factor of ~2.5 for an aspect ratio of 1:4 in the reflector. From that behavior of the partial coherence factor, one concludes that there must be two extreme reflector shapes: one which minimizes the partial coherence factor (and thus maximizes the coronagraphic effect) and one which does the opposite – maximizes the partial coherence factor (and minimizes the coronagraphic effect). These shapes depend on the source's shape, but can be computed for a uniform, circular source by variational calculus by minimizing (maximizing) the expressions for $\Delta(v)$ given in Appendix 3 of ref. 4 for a two-detector intensity interferometer. One then must ask what will happen to the third and higher-order correlations when large reflectors are used. We only made initial calculations which seem to indicate that the multi-aperture coronagraphic effect is far more pronounced, perhaps by orders of magnitude, compared to that obtained with two apertures. Renewed interest in intensity interferometry might justify additional development of this subject.

5. OFF-LINE, MULTI-DETECTOR INTENSITY INTERFEROMETERS

5.1. Off-line processing

The SNR calculated above also scales with the number of optical channels $p^{1/2}$ and electrical bandwidth $b_v^{1/2}$ of the detectors¹. Observations of several targets in a sparse field can be made simultaneously by having a sparse two dimensional detector array mounted on each reflector (similar to atmospheric Čerenkov telescopes), with each point-like source illuminating a different detector where all the j detectors onboard each of the N reflectors point at the same source. The detectors will be further apart than the reflector's point spread function (which will be quite wide, given the crudeness of the reflector).

Recording and offline processing all of data will enable a very productive scientific facility that will measure other observables simultaneously, on top of all quantities derived from precise astrometry:

- 1) Information from all reflectors is gathered simultaneously. The entire correlation function ($N-1$ points) will be measured in a single observation run (on p optical bands). The many (tens and up) baselines will create a dense Fourier plane coverage in a single run, without the need to fit a model to the data. Phases could be recovered by one of the already known and somewhat redundant algorithms^{11,12,15-17}. Imaging will be possible by having sufficient (u, v) coverage (see also §2.2). The proposed instrument will create images with a *minimum* angular resolutions of 1 micro-arcsec (100 elements, each 100m in diameter, so the baseline ≥ 10 km), assuming all the reflectors have no spacing between them, and so probably even significantly better. The ultimate angular resolution limit will probably be set by the longest available baseline, and not by technical difficulty of using it. This accuracy can be compared to GAIA's 10 micro-arcsec and SIM's 1 micro arcsec maximum resolutions.
- 2) Averaging individual reflectors over relatively long periods (seconds) will provide high quality photometry of each target on each of the p optical bands on the same run (N redundant times). This is actually a spectrum with a low, p point, resolution but high quality (high SNR) due to the very large collecting area. Observing several targets simultaneously will enable differential photometry.
- 3) Simultaneous observations in several optical channels will also enable differential interferometry²² to extend even further the dynamical range of the instrument.
- 4) High resolution spectra (within each optical band) of each source can be recovered (N redundant times) by correlation spectroscopy¹⁹.
- 5) Multi-detectors intensity interferometers have an independent capability to measure the distance to each source by searching for the maximum signal¹⁹. This measurement will also give results on the same run (many times: from all

subgroups $\{m\}$ with $|\mathbf{m}| \geq 3$). Assuming we have good knowledge of the distance between the detectors d/c (where c is the speed of light), the relative error of each of the single distance measurements is dominated by the relative lateral (in the plane of the sky) error, as can be seen from¹⁹. Now we can try to take advantage of the fact that we have many individual distance measurements from many subgroups: It is interesting to compare the statistical significance of 1 earth-orbit parallax measurement ($3 \cdot 10^8$ km baseline) and many 1km baseline measurements – which happens at $(3 \cdot 10^8)^2$ individual measurements, or after using all relevant subgroups of an array with just 58 elements. Theoretically, a 100-element array with a 1km typical baseline will measure distances with the same statistical significance as a single measurement with a baseline of 84 light-years. Unfortunately, this is too optimistic since this computation assumes we can detect the distance measurement signal from *each individual* subgroup - which is very difficult already at the 3rd order correlation and quite impossible at the 50th order correlations (as explained above, even for the ~ 100 m diameter reflectors the *total* of all 3rd order correlations is negligible for sources dimmer than magnitude 3, when using NSII technology).

- 6) The high sampling rate of an intensity interferometer, all the way to the GHz scale, will enable the use of the residual timing technique for appropriate sources (for example: pulsars, stellar scintillation, eclipsing objects).
- 7) NSII was already used to measure directly the emergent flux of the source, the source's effective temperature and effect of polarization¹. These observables will also be available to the multi-detector intensity interferometer.
- 8) Multi-photon experiments may uncover thermodynamic information of how the light was originally created or how it has been scattered since its creation²³. A multi-detector intensity interferometer may bring this type of information to the measurable range.
- 9) As a by product, an intensity interferometer can operate as an atmospheric Čerenkov camera. We comment that (a) as a Čerenkov detector, an intensity interferometer might be a bit out of focus as it will be focused to infinity, whereas Čerenkov detectors focus to an altitude of ~ 10 km. (b) Čerenkov radiation will not contaminate long baselines (> 300 m).
- 10) When used for bright sources (not necessarily astronomical sources), this technique can be used as a probe to quantum optics via the pronounced multi-correlation (photon bunching) effect.

Building a completely non-redundant (or only partially redundant) array, in contrast to our fully-redundant array, will only affect the SNR of the reconstructed correlation function, and not the other observables. We also refer to other proposed algorithms related to intensity interferometry improvement:

- Improving the contrast between different parts of the image, and enlarging it without any limitation and, in spite of this enlargement, without any distortions of objects borders caused by discreteness of initial image²⁴.
- Implementation of an eigenfunction method to the problem of correlation function restoration from the photocurrent data²⁵.

Very advanced technology might be required for digitization, computation power and storage. The full analysis of an observation run by an intensity interferometer, as we propose, will be computer intensive. One way this problem may be addressed is with a distributed computing platform such as BOINC (Berkeley Open Infrastructure for Network Computing), which successfully runs several distributed computing projects, of which one is SETI@home²⁶.

5.2. (u,v) Coverage

Since imaging is one of the most important capabilities of any future interferometer, and since the long exposure times necessitate operating in “snapshot” mode (vs. Earth-scan mode), one must consider not just linear configurations but also 2D configurations which cover large parts of (u,v) plane. Consider the configuration depicted in Fig. 3: a double linear equidistant array with spacing d , whose intersection point is between two elements of one of the arms. This type of instrument should be capable of two types of configurations:

When the two arms, each with N reflectors, form a single line, it is optimized for high SNR and dynamical range, acting as a $2N$ linear array, $d/2$ spacing.

When one arm is rotated at an angle with respect to the other: apart from two sets ($N-1$ points each) of high SNR points along each arm, one would get N^2 additional points in the (u,v) plane, equally spaced if the arms are perpendicular, from

inter-arm baselines, but without redundancy for them. This configuration is optimized for geometrically complex objects that require better (u,v) coverage, for a total of $N^2 + 2(N-1)$ different (u,v) points, all observed simultaneously.

For comparison, a completely non-redundant array with $2N$ reflectors would have $N(2N-1)$ different (u,v) points, less than twice the number of baselines as the double linear array, but will have no redundancy whatsoever (with its associated SNR benefits). We note that Herrero²⁷ suggested that a V-shaped array will be the optimal configuration for an intensity interferometer array.

5.3. Realization

It seems that in any case the reflectors will have to be mobile in order to keep the projected separations constant in spite of Earth's rotation, since fixed reflectors would force short integration periods and would render the instrument impotent. Indeed, for this very reason the two NSII reflectors moved on circular tracks during the observations¹. Further simplification may come about by using any of these: mobile focal collector concept employed in radio astronomy, rotating liquid mirrors or the Carlina hypertelescope²⁸. The crude reflectors adversely affect the ability to focus such large reflectors on the relatively small active area of the detectors. This disadvantage may be mitigated by using non-imaging concentrators²⁹, provided that the total path difference after these additional optical elements is not more than the specified tolerance (1cm in our example). Beyond these, we can imagine three major types of realizations: arrays with a central tower, arrays without a central tower, and a cross between the two:

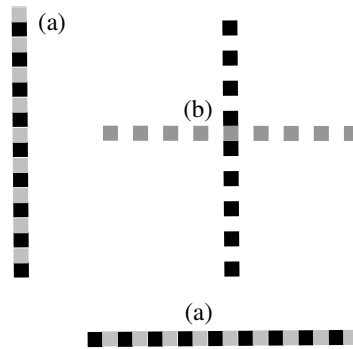


Fig. 3: Two N -redundant linear arrays can be placed at any angle, here they are in-line (a) and at 90° (b).

1) Central tower, as in STACEE (Solar Tower Atmospheric Čerenkov Effect Experiment³⁰): a field of “dumb” mirrors will simply reflect light to a central tower where all light will be detected and processed¹. Advantages: Inexpensive, probably feasible by modifying or nearly replicating a solar tower experiment. The detectors are not mounted on the reflectors, so all the sensitive electronics of the entire instrument are fixed, protected and easily accessible, Almost flat reflectors, Shorter electrical leads from detection to recording. Disadvantages: Due to the poor optical quality of the reflectors and the large distance to the tower, probably only one target per observation will be possible, Atmospheric extinction of the signal and scintillation along the way from the mirrors to the tower.

2) No central tower, as in NSII: every reflector will carry all its detectors onboard. Advantages: The short reflector-detector distance enables multi-targeting, No atmospheric extinction or scintillation from the reflectors to detectors. Disadvantages: Cannot be realized on any existing array (including astronomical arrays observing at the mm or longer wavelengths), without major modifications, and probably would have to be a dedicated instrument, Will create a need to protect the detectors from the elements on many separate and mobile platforms.

3) A cross of the two may be possible: instead of placing a detector on every reflector on the NSII-like configuration, a light guide is positioned at the focus, for example, a multimode optical fiber or a bundle thereof, bringing the signals all the way to a central, fixed, lab. Advantages: it eliminates all the disadvantages of the two configurations above, except the need to build it probably as a dedicated facility. It might be relatively inexpensive. Disadvantages: the poor optical quality of the reflector may require non-imaging optics to collect the light into the light guide.

As a short-term goal, we think that the best place to start is STACEE by augmenting it with much more data storage capability (hours of real-time data, instead of the current ~ 100 nanoseconds). In practice, some work will also be done in order to eliminate any zero-point drifts of the detectors to a very high degree of accuracy. We think that STACEE is a prime candidate for early experiments to validate the results of this work since it already has a field of uniformly spaced (albeit fixed) reflectors, all the electronics of high-speed detection of light from specific reflectors, and of course, the fact that it is already build, so capital investment will be minimal indeed. Although the 37m^2 area of each of the 220 heliostats may seem too small, this limitation can be overcome by combining the detected intensity of several adjacent heliostats to simulate a single large reflector (after correcting for geometric path difference), and thus the whole field can simulate a few very large reflectors. This setup may also help to mitigate the focusing mismatch between atmospheric Čerenkov cameras and intensity interferometers. After this work was accomplished^{20,31,32}, a more limited proposal was also raised following the same lines³³.

Among many others, two special targets may utilize the capabilities of intensity interferometry to the fullest:

- Fast repeaters (such as pulsars): as in boxcar averaging, binning the few-GHz of samples into millisecond bins, synchronized with the pulsar's period, will provide a way to create a "movie" of the different phases of the Pulsar. The cost: observing time will scale by the number of frames in the "movie".
- Close binaries and multiples, including bright compact objects and extra-solar planets: these will be found and characterized by astrometry (from interferometry and imaging), radial velocity (from high resolution spectra), photometry (transits and lensing events), and residual timing, all independently and in the same observational run.

One of the appeals of the proposed instrument is that no new technology needs to be developed and all the components (besides the reflectors themselves) are off-the-shelf products. Yet, we can say what kind of technological advance would further promote this kind of instrument significantly: since the only uncontrolled parameter of the exponential factor $NA\alpha n$ is the spectral flux density n , then theoretically one would want to have a device that optically amplifies the intensity of the source before it is electronically detected, in front of every detector. The difficulty is that this device needs to operate at high speed, uniformly (for all detectors) and while keeping all the statistical properties of the light to allow for post-processing of the data. We note that amplification of an optical signal always involves its absorption first, and thus the above advantages can currently only be realized at much longer wavelengths ($\lambda \geq 30\mu\text{m}$), where off-line amplitude interferometers, with their superior sensitivity, might be feasible.

6. CONCLUSIONS

We presented an algorithm for the improvement of the SNR of an evenly spaced off-line multi-detector intensity interferometer by utilizing its very high redundancy. We showed that by stacking many contributions in the multi-correlation regime the SNR of such an array scales approximately exponentially with $(NA\alpha n)$ (fig. 2 top curve). We demonstrated the algorithm on the simplest term $F^{(2)}(\tau_1, \tau_2)$ but the generalization to triple and higher correlation is straightforward. We showed that translational symmetry improves the performance of the instrument by a factor of about five, and that multi correlation can further improve that performance significantly (a total improvement of more than 190-fold), under the investigated conditions. This improvement is made possible by the offline processing of the data that allows us to "use" each photon several times and thus to alleviate the low intrinsic sensitivity of intensity interferometers, to achieve a limiting magnitude of about 14.4 magnitudes, when using 100-element, 7680m^2 each, conservatively technologically improved array. Indeed, off-line processing of the data enables to reconstruct the whole complex correlation function (in $N-1$ points) from a single observation run by using all available $F^{(m)}(\{m\})$. Since the number of detectors N is expected to be at least few dozens, the (u, v) coverage will be good enough to reconstruct an optical interferometric image with resolution in the μs range (100 elements, each 100m in diameter means a *minimum* baseline of 10Km) without having to fit the visibility curve to some model. Offline processing of the data will also enable measuring a variety of other observables, including photometry, spectroscopy, distance and timing, and thus to create a very productive astronomical facility.

Using all of these properties will enable the relatively simple construction of a ground based facility able to transform a $2D$ field of point-like sources to a $3D$ distribution of micro-arcsec resolved systems. Each of the systems will be truly imaged in p optical bands without a need to fit the visibility curve to some model, and it will also have its high quality spectra (inside each optical band), photometry, emergent flux, effective temperature, high resolution residual timing and

polarization effects measured. All of these can be achieved in a single observation run of such a dedicated facility. The facility will not need adaptive optics, beam combiners, delay lines, precision optics and mechanics of almost any kind. In addition, due to their mechanical robustness intensity interferometers are far more amenable to use in shorter wavelength, and indeed NSII already operated at the blue band at 438.4nm.

The above-mentioned properties may warrant an evaluation of such a facility as an alternative to space interferometer missions (such as SIM³⁴). The proposed instrument might outperform SIM in many parameters: it will have far better resolution, more observables, it will create images for all observed objects, it presents a much simpler technological challenge, and it will be ground-based.

Admittedly, the proposed instrument is big: 100 elements, each ~100m in diameter is not a simple thing to call for. Yet, it is very well within current technical capabilities as all of the requirements are already well-exceeded by different currently operating or already-planned instruments: STACEE is already using some of the 220 digitally-controlled 37m² heliostats for optical detection at 1 GHz, The Green Bank Telescope is a single aperture that already boasts 7853m² of collecting area, accurate to better than 0.22mm rms³⁵, compared to 7680m² accurate to 1cm that we used in our calculations, and the total scale of the proposed instrument (768,000m² active area) is smaller than the proposed 10⁶ m² of the Square Kilometer Array at comparable mechanical accuracy³⁶. We did not make any cost assessments for the construction of such a facility, but we recognize that cost will be a crucial issue for such a major facility.

Contemporary astronomy is plagued by the need to have optical surfaces smooth and distances fixed to a fraction of the wavelength. Multi-detector optical intensity interferometry offers a way out of this restriction, even if not for the faintest of objects, offering:

- Ease of construction since mechanical accuracy depends on electrical bandwidth, and not on wavelength. Using mobile focal collectors may significantly reduce the moving mass of each reflector.
- All reflectors are identical and are not connected optically to the others. Furthermore, reflectors will probably be segmented, enabling "industrialized" parts manufacturing.
- Relatively easy to obtain very long baselines of many kilometers at 1cm mechanical accuracy.
- No new technological development is needed.

After 35 years, results obtained with intensity interferometry are still the state of the art, resolution-wise, and especially so in the blue, where amplitude interferometry is lacking. The main drawback of intensity interferometry is sensitivity, but using all of the proposed improvements and scaling laws improves the limiting magnitude from 2.5 at NSII to 14.4 of the proposed instrument. It seems that multi-detector intensity interferometry could be used as a present day technique answering present day questions, and indeed deserves another review.

This work is based upon a master's thesis by A. Ofir³¹. Parts of this work were supported by the European Interferometry Initiative through OPTICON (an EU Framework VI program).

REFERENCES

1. Hanbury Brown R, *The intensity interferometer – its application to astronomy*, Taylor & Francis LTD., 1974.
2. Hanbury Brown R., Jennison R. C. Das Gupta, M. K., Apparent angular sizes of discrete radio sources, *Nature* 170, 1061 (1952).
3. Hanbury Brown R. Twiss R. Q. Interferometry of the intensity in light fluctuations. I. Basic theory: the correlation between photons in coherent beams of radiation, *Proc. R. Soc. A* 242, 300 (1957).
4. Hanbury Brown R., Twiss R. Q., Interferometry of the intensity fluctuations in light. II. An experimental test of the theory for partially coherent light, *Proc. R. Soc. A* 243, 291 (1957).
5. Baym G., The physics of Hanbury Brown Twiss intensity interferometry: from stars to nuclear collisions, *Acta Physica Polonica B* 29, 1839 (1998).
6. Bussian D.A. *et al.*, Photon pair correlation spectroscopy of single tetrahedraloligophenylenevinylene molecules at room temperature, *Chemical Physics Letters* 388, 181 (2004).
7. Yabashi M., Tamasaku K., Ishikawa T., Characterization of the transverse coherence of hard synchrotron radiation by intensity interferometry, *Phys. Rev. Lett.* 87, 14, id. 140801 (2001).

8. Liu X., Clegg W. W., Liu B., Interferometry method for measuring head-disk spacing down to contact, *Proc. SPIE* **3740**, 598 (1999).
9. Sattler S. Hartfuss H. J., Intensity interferometry for measurement of electron temperature fluctuations in fusion plasmas, *Plasma Phys. Control. Fusion* **35**, 1285 (1993).
10. Qian H., Elson E. L., Fluorescence correlation spectroscopy with high-order dual-color correlation to probe nonequilibrium steady states, *PNAS* **101**, 2828 (2004).
11. Bartelt H., Lohmann A. W. W. W. Wirnitzer B., Phase amplitude recovery from bispectra, *Appl. Opt.* **23**, 3121 (1984).
12. Lohmann A. W. W. Wirnitzer B., Triple correlations, *Proc. of the IEEE* **72** 7 889, 1984.
13. Gamo H., Triple correlator of photoelectric fluctuations as a spectroscopic tool, *J. App. Phys.* **34**, 875 (1963).
14. Sato T., Wadaka S., Yamamoto J., Ishii J., Imaging system using an intensity triple correlator, *Appl. Opt.* **17**, 2047 (1978).
15. Marathay A. S., Hu Y. Shao L., Phase function of spatial coherence from second-, third-, fourth order intensity correlations, *Opt. Eng.* **33**, 3265 (1994).
16. Barakat R., Imaging via the van Cittert Zernike theorem using triple-correlations, *J. Modern Opt.* **47**, 1607 (2000)
17. Mendlovic D., Mas D., Lohmann A. W., Zalevsky Z. Shabtay G., Fractional triple correlation and its applications, *J. opt. Soc. Am. A* **15**, 1658 (1998).
18. Holmes R. B. Belen'kii M. S., Investigation of the Cauchy–Riemann equations for one-dimensional image recovery in intensity interferometry, *J. Opt. Soc. Am. A* **21**, 697 (2004).
19. Fontana P. R., Multidetector intensity interferometers, *J. Appl. Phys.* **54**, 473 (1983).
20. Ofir A. and Ribak N. E., Off-Line, Multi-Detector Intensity Interferometers I: Theory, *MNRAS*, Accepted (2006).
21. Twiss R. Q., Applications of intensity interferometry in physics astronomy, *Optica Acta* **16**, 423 (1969).
22. Vannier M., Petrov R. G., Lopez B., Differential interferometry detection and spectroscopy of extra solar planets with VLTI. *Société Française d'Astronomie et d'Astrophysique conference*, Lyon, France (2001).
23. Dravins D., Hagerbo H. O., Lindgren L., Mezey E., Nilsson B., Optical astronomy on milli-, micro-, and nanosecond timescales. *Proc. SPIE* **2198**, 289 (1994).
24. Telyatnikov A. A., Complex method of image restoration for compressed optical information quality improvement. *Proc. SPIE* **3317**, 69 (1997).
25. Kurashov V. N., Kurashov A. V., Piskarev V. L., Restoration of light correlation function from the data of delayed photocounts in intensity interferometry. *Proc. SPIE* **3317**, 36 (1997).
26. Korpela Eric J. et al, Three Years of SETI@home: A Status Report. *Bioastronomy 2002: Life Among the Stars*, *Proc. IAU Symposium* **213**. Ed. R. Norris, F. Stootman. San Francisco: Astron. Soc. Pac., 419 (2003).
27. Herrero V., Design of optical telescope arrays for intensity interferometry. *Astroph. J.* **76**, 198 (1971).
28. Le Coroller H, Dejonghe J., Arpesella C., Vernet D., Labeyrie. A., Tests with a Carlina-type hypertelescope prototype. *Astronom. Astroph.* **426**, 721 (2004)
29. Gleckman P., O'Gallagher J. & Winston R., Concentration of sunlight to solar-surface levels using non-imaging optics. *Nature* **339**, 198 (1989).
30. Covault C. E. et al, The status of the STACEE Observatory. *Proc. 27th International Cosmic Ray Conference*. Hamburg, Germany. (2001).
31. Ofir A., *The properties of the off-line, multi-detector intensity interferometer*, M.Sc. thesis, Raymond Beverly Sackler Faculty of Exact Sciences, Tel Aviv University, Tel Aviv, Israel, 2005.
32. Ofir A. and Ribak N. E., Off-Line, Multi-Detector Intensity Interferometers II: Implications and Applications, *MNRAS*, accepted (2006).
33. LeBohec S., Holder J., Using atmospheric Cherenkov telescope arrays as intensity interferometers. eprint arXiv:astro-ph/0507010. Submitted, *29th International Cosmic Ray Conference*, Pune (2005).
34. Boker T., Allen R. J, Imaging and nulling with the Space Interferometer Mission. *Astroph. J. Suppl.* **125**, 123 (1999).
35. Jewell P. R., Langston, G. The Green Bank telescope: an overview, *Astrophysical Phenomena Revealed by Space VLBI. Proc. VSOP Symposium*, Kanagawa, Japan, Eds. H. Hirabayashi, P.G. Edwards, D.W. Murphy, Institute of Space and Astronautical Science, 297 (2000).
36. Carilli C., Rawlings S., Science with the Square Kilometer Array: motivation, key science projects, standards and assumptions. arXiv:astro-ph/0409274 (2004).